Thermoelectric Hall conductivity of fractional quantum Hall systems on a disk

Zi-Yi Fang,[1] Dan Ye,[1] Yu-Yu Zhang,[1,2,*] and Zi-Xiang Hu[1,2,†]

[1]*Department of Physics, Chongqing University, Chongqing 401331, People's Republic of China*

[2]*Chongqing Key Laboratory for Strongly Coupled Physics, Chongqing 401331, People's Republic of China*

(Received 1 February 2021; revised 14 June 2021; accepted 16 June 2021; published 25 June 2021)

For fractional quantum Hall states on a finite disk, we study the thermoelectric transport properties under the influence of the presence of an edge and its reconstruction. In a recent study on a torus [Phys. Rev. B **101**, 241101(R) (2020)], Sheng and Fu found a universal non-Fermi liquid power-law scaling of the thermoelectric conductivity $\alpha_{xy} \propto T^{\eta}$ for the gapless composite Fermi liquid state. The exponent $\eta \sim 0.5$ appears an independence of the filling factors and the details of the interactions. In the presence of an edge, we find the properties of the edge spectrum dominants the low-temperature behaviors and a nonuniversal scaling behavior in low temperature is observed. To consider individually the effect of the edge states, the real space entanglement spectrum of the model wave function, which contains only the spectrum of edge excitation is employed. Its spectrum energies could be tuned by varying the radius of the subsystem. In the non-Abelian Moore-Read state, the Majorana neutral edge mode is found to have more significant effects than that of the charge mode in the low temperature.

DOI: 10.1103/PhysRevB.103.235161

I. INTRODUCTION

When the strongly interacting two-dimensional electron gas (2DEG) is exposed in a perpendicular strong magnetic field and extremely low temperature [1], the formed fractional quantum Hall (FQH) state reveals the nontrivial topological properties, such as fractional charge excitations and fractional statistics [2]. Some of the FQH states [3] could have non-Abelian fractional excitations and relevant edge modes. In a FQH state, the bulk is a gapped insulator and the low-lying excitation in the bulk is the neutral magnetoroton excitation [4], which could be described as separating pairs of the particle-hole excitations [5]. Furthermore, in a realistic Hall bar sample which is usually applied to measure the conductance of FQH state, the existence of an open boundary is usually unavoidable. The edge physics plays an essential role to uncover the bulk topological properties due to the so-called bulk-edge correspondence [6,7]. On the edge of a FQH droplet, the description of Fermi liquid theory is broken down and the interacting electrons prefer to form a chiral Luttinger liquid (CLL) [8]. For a Laughlin state at filling factor $\nu = 1/m$, the action of the chiral edge excitation [8] is

$$\mathbf{S} = \frac{m}{4\pi} \int dt dx (\partial_t + v\partial_x)\phi\partial_x\phi, \tag{1}$$

where the $\phi(x,t)$ is the chiral (right moving) bosonic field. The velocity of edge excitation v is a boundary effect which is determined by the edge potentials. Therefore, the edge velocity is actually an external parameter that is not contained in the intrinsic topology. It is theoretically predicted that the current-voltage dependence in the tunneling between a Fermi liquid and a quantum Hall edge obeys a universal power-law $I \sim V^m$ [9]. Such universality, however, has not been conclusively observed in experiments. A very likely reason is the occurrence of additional nonchiral edges that are not tied to the bulk topology [10], namely, the edge reconstruction, which is a consequence of the competition between the positive background confinement potential and electron-electron Coulomb repulsive interaction [11–14]. It induces nonchiral edge modes and thus breaks the CLL description. In spite of its nonuniversality, one of us recently found that in the entanglement spectrum, which represents the virtual edge excitations of the reduced density matrix in a bipartite wave function, still can be tuned and reconstructed by varying the radius of the subsystem [15].

Since the edge excitation is gapless and has lower energy than that of the neutral magnetoroton excitation in the bulk, intuitively, it dominates the low-lying energy behavior of the system, regardless of the charge or heat transport experiments. Moreover, while the back scattering between two nearest neighboring charged modes occurs, a charged neutral mode could appear, such an example is the $\nu = 2/3$ state [16,17]. In a non-Abelian FQH state, such as the Moore-Read state at $\nu = 5/2$, a Majorana neutral mode exists which is the heart of its non-Abelian topology. Because of the charge neutrality, these neutral edge modes can not be detected directly by electrical measurements. Then the thermoelectric phenomena that provides the direct conversion between heat and electricity is interesting and useful. In a thermoelectric measurement, one sets up a temperature gradient ∇T, and an electrical current I is generated by the system to compensate for its effect. They are related to each other by $I_i = -\alpha_{ij}\nabla_j T$ where α_{ij} is the thermoelectric conductivity. Experimentally, one usually

*yuyuzh@cqu.edu.cn
†zxhu@cqu.edu.cn

measures the thermopower S_{xx} and Nernst coefficient S_{xy} and they are related to α_{ij} by $S_{ik} = \alpha_{ij}\rho_{jk}$, in which ρ is resistivity. It is known that the thermoelectric response is directly related to thermal entropy per electron [18–21]. Because of the huge degeneracy of the non-Abelian FQH states with quasiparticle excitations, it was proposed to probe the non-Abelian statistics of the quasiparticles and measure their quantum dimension [22,23]. Very recently, it is shown that two-dimensional quantum Hall systems can reach thermoelectric figure of merit on the order of unity down to low temperature, as a consequence of the thermal entropy from the massive Landau level (LL) degeneracy without considering the Coulomb interaction [24].

For a Fermi liquid, since the entropy is associated with the number of thermal excitations within k_BT near the Fermi energy, a linear T dependence has been conjectured [25,26]. While including the Coulomb interaction, the LL degeneracy is lifted, and FQH states are formed at specific fillings factors. In that case, the electron system is a non-Fermi liquid and the ground state has only the degeneracy due to the center of mass translational symmetry in a translational invariant system. In Ref. [27], Sheng and Fu calculated the α_{xy} for FQH system in a torus geometry. A non-Fermi liquid pow-law scaling $\alpha_{xy} \propto T^{\eta}$ with $\eta \sim 0.5$ for composite Fermi liquid states at $\nu = 1/2$ and $\nu = 1/4$ was found. α_{xy} vanishes exponentially $\alpha_{xy} \sim \exp(-\Delta/k_BT)$ with a neutral magnetoroton gap for $\nu = 1/3$ Laughlin FQH state while $T \to 0$. However, as we stated above, the low-lying energies of the FQH system are dominated by the edge states in system with a boundary which was neglected in the torus geometry. They should naturally have contributions in the low-temperature transport. In this work, we consider the thermoelectric conductivity in disk geometry to see how does the edge state and its reconstruction affect the thermoelectric conductivity, especially the low-temperature scaling behavior. To isolate the effect of the edge excitations, the real space entanglement spectrum of the model wave function is used to calculate the α_{xy} for considering the virtual edge excitations along the boundary of the subsystem. We will show that the edge, and its reconstruction result in a nonuniversal non-Fermi liquid scaling behaviors in low temperature. The Majorana edge mode in Moore-Read state is found to be important for the low-temperature measurements.

The rest of this paper is organized as following: In Sec. II, we compare the thermoelectric conductivity results from energy spectrum with and without edge states. The dipolar fermions in FQH and trivial phases are also considered. In Sec. III, the real space entanglement spectrum is used to analyzing the effect of the edge states. The non-Abelian FQH state and the dependence of α_{xy} are also considered, and Sec. IV gives the conclusions and discussions.

II. COMPARING DIFFERENT GEOMETRIES AND PHASES

Since the thermoelectric conductivity is directly related to the thermal entropy per electron, we perform a full diagonalization in a finite system at a given filling factor. The eigen-energies are used to calculate the partition function Z at a given temperature T,

$$Z = \sum_i \exp(-E_i/k_BT). \tag{2}$$

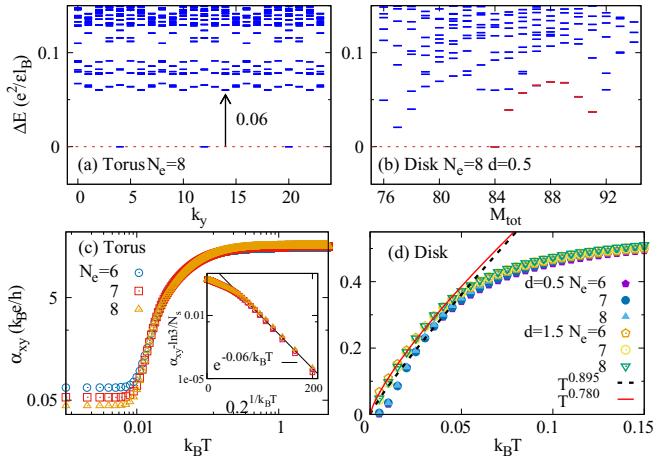

FIG. 1. The energy spectrum for 8 electrons in 24 orbitals with Coulomb interaction on torus (a) and disk (b). k_y is the center-of-mass momentum in y direction on torus and M_{tot} is the total angular momentum in z direction on disk. In panel (b), the positive confinement is set at a distance $d = 0.5\ell_B$ from electron layer. The gapless edge mode dispersion is labeled by red color. Panels (c) and (d) depict the α_{xy} (in units of k_Be/h) versus the thermal energy k_BT in units of $e^2/\epsilon\ell_B = 1$ for 6–8 electrons at $\nu = 1/3$. In the inserted plots in panel (c), we fit the low-temperature data with $\alpha_{xy} \sim \exp(-\Delta/k_BT)$. In panel (d), two confinement potentials are used. $d = 0.5\ell_B$ is in the Laughlin phase and $d = 1.5\ell_B$ is in the edge reconstructed phase.

Then the thermal entropy can be obtained as

$$S = -\sum_i \rho_i \ln \rho_i, \tag{3}$$

with $\rho_i = \exp(-E_i/k_BT)/Z$ the probability for the ith state to be occupied at temperature T and E_i the eigen-energies. In the absence of disorder, thermoelectric Hall conductivity α_{xy} is proportional to the entropy density as

$$\alpha_{xy} = \frac{s}{B} = \frac{S}{N_{\text{orb}}}, \tag{4}$$

where N_{orb} is the number of orbitals for electrons occupying in a given Landau level and s is S divided by the area of 2DEG which is $2\pi\ell_B^2 N_{\text{orb}}$. Here ℓ_B is the magnetic length $\ell_B = \sqrt{\hbar c/eB}$. Suppose the dimension of the Hilbert space is Ω, in high temperature limit such that the thermal activation overwhelms all the energy scale of the many-body system, such as the neutral gap or quasiparticle excitation gap in the bulk, namely $k_BT \gg \Delta$. Each eigenstate has identical probability $\rho_i = 1/\Omega$, and thus the thermal entropy is classical $S = \ln\Omega$. In this case, $\alpha_{xy} = \ln\Omega/N_{\text{orb}}$ is a constant. For a state with N_e electrons at filling $\nu = N_e/N_{\text{orb}}$, the dimension of the Hilbert space, which is just a binomial $\Omega = C_{N_{\text{orb}}}^{N_e}$, reaches its maximum at $\nu = 1/2$ and thus the half filling has the largest α_{xy}. It has potential to enable thermoelectric cooling and power generation with unprecedented efficiency [24].

At low temperature, as shown in Fig. 1, we compare the results on torus with that on disk. For Coulomb interaction at $\nu = 1/3$, the energy spectrum on torus has threefold degeneracy due to the center-of-mass translational symmetry. In this case, the threefold degenerated ground states are gapped by neutral magnetoroton excitation in the bulk [19].

In disk geometry, mimicking the 2DEG in semiconductor GaAs-GaAlAs hetero-structure, we diagonalize a Hamiltonian which contains the 2DEG and a homogeneous positive background confinement potential [11,12]. The background potential origins from the δ-doping layer at a distance d from the electron layer which is treated as homogeneous with density σ. Then the electron on the mth orbital feels the confinement energy $U_m = \langle m|\frac{e\sigma}{\sqrt{d^2+r^2}}|m\rangle$. As shown in Fig. 1(b), the ground state is unique and a chiral gapless edge excitation (its lowest branch are in red) dominates the low-lying energy spectrum in thermodynamic limit. As a result, the thermoelectric Hall conductivity α_{xy} at low temperature exhibits different behaviors in two cases. In Fig. 1(c) which was also shown in Ref. [27], the α_{xy} is saturated at a value $\ln 3/N_{\rm orb}$, while $T \to 0$ due to the threefold ground-state degeneracy. For a gapped phase on torus, the low-temperature data before saturation could be fitted by $\exp(-\Delta/k_BT)$ as shown in the inserted plot. Δ is actually the neutral gap which is labeled by arrow in Fig. 1(a). In disk geometry, as shown in Fig. 1(d), the α_{xy} for $\nu = 1/3$ FQH state has a similar behavior as that for the composite Fermi liquid at $\nu = 1/2$ and $\nu = 1/4$ on torus. It approaches to zero while $T \to 0$. After neglecting the data below the average energy gap in the spectrum, which origins from the finite-size effects, we fit the low-temperature data using $\alpha_{xy} \propto T^{\eta}$ with $\eta \simeq 0.895$ for $d = 0.5\ell_B$ and $\eta \simeq 0.780$ for $d = 1.5\ell_B$. The reason to take these two cases is that the Laughlin-like ground state which has total angular momentum $M_{\rm tot} = 3N_e(N_e-1)/2$, only survives as the global ground state in window $d \in [0, 1.35]\ell_B$ (for 8 electrons). When $d \sim 1.5\ell_B$, the ground-state angular momentum is changed and the edge reconstruction occurs. Here we notice that for a given d, the data for different system sizes collapse on to one curve which demonstrates a small finite-size effect. Therefore, in the presence of edge, we find varying confinement potential significantly changes the low-temperature scaling behavior of the α_{xy}.

As another example to see the different low-temperature behaviors of α_{xy} in gapped and gapless phases, we consider the dipole-dipole interaction for degenerate quantum gas in a fast rotating trap [28]:

$$V_{dd}(\vec{r},\theta) = \frac{r^2 - 3(z\cos\theta + x\sin\theta)^2}{r^5}, \tag{5}$$

where θ is the angle between the dipole moment and the z axis. In a fast rotating limit at which the rotating frequency is close to that of the harmonic trap potential, the system enters into the quantum Hall regime [28]. It was found [29–31] that the Laughlin phase robustly survives while the tilting angle θ is small. As the θ is increased, the ground-state gap is gradually reduced and finally closed, then the system enters into a cluster state [30] because of the anisotropic attractive interaction in one direction. The interaction in Eq. (5) could be rearranged as

$$V_{dd}(\vec{r},\theta) = \frac{3\cos^2\theta - 1}{2}\frac{r^2 - 3z^2}{r^5} + \frac{3\sin^2\theta}{2}\frac{y^2 - x^2}{r^5}. \tag{6}$$

The first term is isotropic and the second term is anisotropic in the 2D plane. The magic angle $\theta = 54.7^\circ$ satisfies the condition $3\cos^2\theta - 1 = 0$, at which the interaction only contains the second term. In Fig. 2(a), we plot the energy gap between the lowest two states via diagonalizing Eq. (6) on torus for several system sizes. The extrapolation in thermodynamic limit from finite-size scaling clearly tells us the system is gapped for $\theta = 0^\circ, 30^\circ$ and gapless for $\theta = 54.7^\circ, 90^\circ$, respectively. In Figs. 2(b) and 2(c), we plot the α_{xy} for $\theta = 0^\circ$ and 54.7° which are in two different phases. The α_{xy} in FQH gapped phase is similar to that of the Coulomb Hamiltonian in Fig. 1(a) and the low-temperature part still satisfies $\alpha_{xy} \sim \exp(-\Delta/k_BT)$. However, in a topological trivial gapless phase at 1/3 filling, as shown in Fig. 2(c), we find the low-temperature behavior could be fitted by $\alpha_{xy} \sim T^{0.97}$, which is very close to the Fermi liquid exponent $\eta = 1$. Therefore, from low-temperature thermoelectric Hall conductivity, we speculate the phase transition in dipolar fermions is a topological phase to Fermi liquid transition.

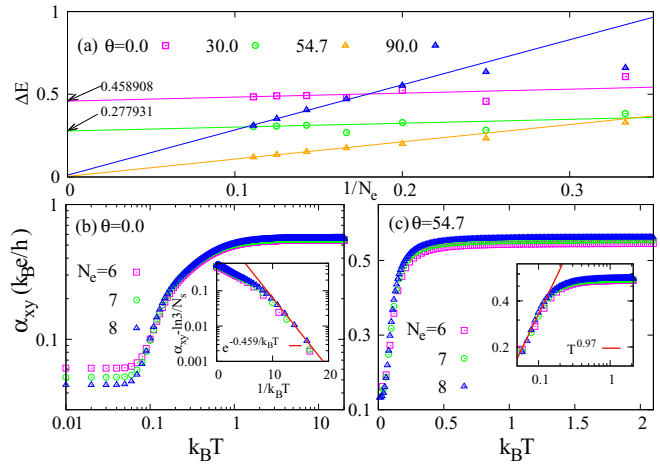

FIG. 2. For fast-rotated dipolar fermions on a torus, finite-size scalings of the ground energy gap at different titled angles θ for the dipole moment. The particle number is 8 and the thickness in z direction is set to $q = 0.01$ in unit of $l = \sqrt{\hbar/(2\mu\omega)}$ where μ is the effective mass and ω is the frequency of the trap potential. $\theta = 54.7^\circ$ is the magic angle at which the dipole-dipole interacting is purely anisotropic and the system is gapless. More details are in Ref. [29]. Panels (b) and (c) depict the α_{xy} and fittings for 6–8 particles at $\theta = 0^\circ$ and $\theta = 54.7^\circ$. The gapless phase shows the Fermi liquid behavior with $\eta \simeq 1$.

Based on the results of above two cases, we suspect that the existence of the gapless edge mode or gapless trivial phase could have different scaling exponent of the thermoelectric Hall conductivity in low temperature.

III. THE EFFECTS OF PURE EDGE STATES

In previous section, we observe that the presence of an edge significantly changes the low-temperature behaviors of the thermoelectric Hall conductivity. In the energy spectrum, we always have both the bulk states and the edge states. To individually consider the effect of the edge states, we calculate α_{xy} for the real space entanglement spectrum [32–34] of a model wave function. To be precise, a bipartition of a quantum system is defined when the Hilbert space is divided into two subsystems, $H = H_A \bigotimes H_B$. Then a Schmidt decomposition

is performed to the ground state [35,36]:

$$|\Psi\rangle = \sum_i e^{-\frac{1}{2}\xi_i} |\psi_A^i\rangle \bigotimes |\psi_B^i\rangle, \tag{7}$$

where the $\exp(-\xi_i) = \lambda_i$ are the eigenvalues of the reduced density matrix of subsystem $\rho_A = \mathrm{Tr}_B|\Psi\rangle\langle\Psi|$. It is normalized by $\sum_i e^{-\xi_i} = 1$. If ρ_A has finite dimension, the von Neumann entanglement entropy is defined as $S_A = -\sum_i \lambda_i \log\lambda_i = \sum_i \xi_i \exp(-\xi_i)$. It was known by Haldane [37] that the full structure of the "entanglement spectrum" (ES), which is the logarithmic Schmidt spectrum of level ξ_i, contains much more information about the entanglement between two halves than that from S_A only. It plays a key role in analyzing the topological order of the FQH state. The structure of ES is analogous to the low energy excitations of a many-body Hamiltonian [6,7]. Especially, for the model wave function, the ES only contains the edge state (CFT state). The counting number per momentum sector of ES is identical to that of the edge spectrum in CLL theory. Beyond the counting, one of us [15] recently found that the entanglement spectrum in real space cut appears the signals of edge reconstruction via tuning the area of the subsystem. The edge velocity reaches its minimum when the area of subsystem is equal to that of the correlation hole. For example, for a subsystem with N_A electrons, while the radius of subsystem R_A is changed, the energies of the ES are changed although the counting numbers are invariant. The energy with momentum $M_0 + N_A$ is smaller than that of the Laughlin state at momentum M_0 when $R_A = \sqrt{2N_A/\nu}$. We called it ES reconstruction since the similar phenomena happens in the real edge density reconstruction as shown in Refs. [11,12].

We consider the $\nu = 1/3$ Laughlin wave function for 10 electrons on a disk which can be obtained either from diagonalizing a V_1 pseudopotential hamiltonian [38] or from the Jacks polynomial recipe [39,40]. Because the bipartition we used conserves the rotational symmetry, the ES for a given number of electrons in subsystem N_A and radius of the circular cut R_A are shown in Figs. 3(a) and 3(b). Here we consider the subsystem contains four particles and the radius of the subsystem R_A is a parameter we tuned. It shows that the ES for the same N_A and different R_A have different spectra. Consequently, their thermoelectric Hall coefficient α_{xy} have different behaviors at low temperature as shown in Figs. 3(c) and 3(d), respectively. To eliminating the finite-size effect, we still fit the low-temperature data above the typical average energy interval. The exponent are $\eta \simeq 0.973$ and $\eta \simeq 0.753$ for two cases, both of which are larger than $\eta \simeq 0.5$ on torus and smaller than that of the Fermi liquid value. Therefore, the FQH edge states still possess non-Fermi liquid characteristics, but its scaling exponent could be changed by tuning the edge velocity (slope of the dispersion near $k \sim 0$) and thus nonuniversal.

Now let us move to the non-Abelian FQH state which has a more complicate edge structure. One prominent example is the Moore-Read state [41] which is one of the candidate ground-state description for $\nu = 5/2$ filling in the second Landau level. Its model wave function could be obtained from diagonalizing a three-body V_3 pseudopotential [42] Hamiltonian or Jack polynomials. The subscript 3 is the relative angular momentum of three-body interacting particles.

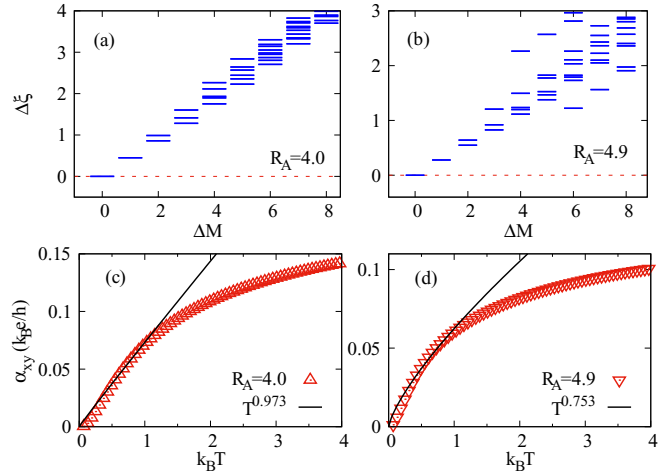

FIG. 3. The real space ES for subsystem of $N_A = 4$, $R_A = 4.0\ell_B$(a) and $R_A = 4.9\ell_B$(b) for a 10-electron Laughlin state. N_A and R_A is number of electrons and radius of the subsystem. The typical energy level spacing is defined as the gap between the lowest two states. ΔM is the angular momentum difference between the excited and ground state. Panels (c) and (d) depict the α_{xy} and low-temperature fittings from the spectrum panel (a) and panel (b) correspondingly.

Figure 4(a) depicts the ES for 12-electron Moore-Read state. Unlike the Laughlin state, the counting numbers of edge spectrum becomes to be 1, 1, 3, 5 . . . . This is due to the existence of a neutral Majorana mode in addition to the bosonic charge mode [43]. Figure 4(b) depicts the energy spectrum of a mixed Hamiltonian

$$H = (\lambda - 1)H_{2B} + \lambda H_{3B}, \tag{8}$$

with $\lambda = 0.5$ for 12 electrons with different confinements. We label the edge states (blue) and bulk states (green) in

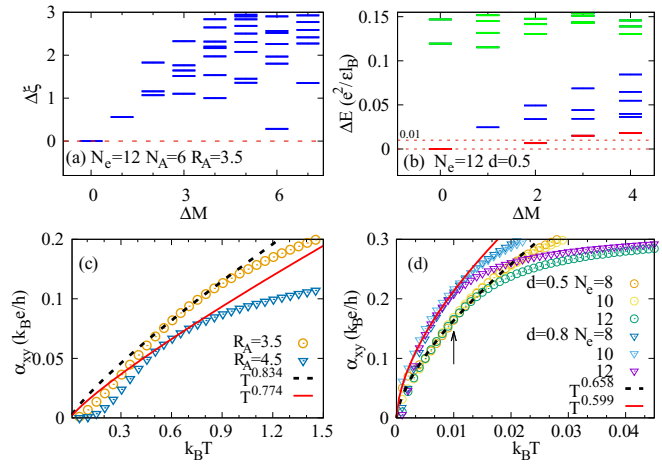

FIG. 4. (a) ES for $N_A = 6$ and $R_A = 3.5$ in a 12-electron Moore-Read state. (b) The low-lying energy spectrum of a mixed Hamiltonian Eq. (8) with $\lambda = 0.5$ for 12 electrons with $d = 0.5\ell_B$. The lowest branch of Majorana mode which has one order lower energy than that of the bosonic charge mode has been labeled in red. In panels (c) and (d), we plot the α_{xy} versus $k_B T$ for panels (a) and (b), respectively, with different parameters.

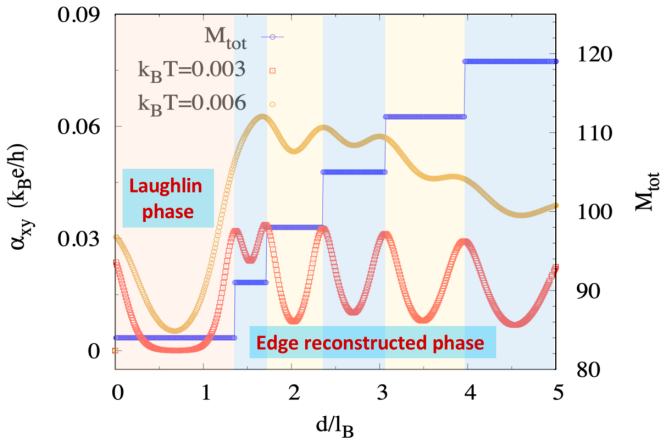

FIG. 5. The ground-state quantum number $M_{\rm tot}$ and low temperature α_{xy} as varying d/ℓ_B for 8 electrons at $\nu = 1/3$. The peak of α_{xy} corresponds to the ground-state phase transition or the edge reconstruction.

different colors. In Eq. (8), H_{2B} contains the electron-electron Coulomb interaction and confinement potential and H_{3B} is the three-body model Hamiltonian. The reason of mixing H_{3B} is to separate the ground state and edge states from bulk states since the edge mode has zero energy in pure three-body Hamiltonian ($\lambda = 1$). The lowest branch of Majorana mode is labeled in red color. Figures 4(c) and 4(d) show their corresponding α_{xy} in low temperature. For the ES, we have $\eta \simeq 0.834$ and $\eta \simeq 0.774$ for $R_A = 3.5$ and 4.5, respectively. Just like the case of Laughlin state, tuning the area of the subsystem or the edge velocities changes the scaling exponent η. For the energy spectrum, we plot the α_{xy} for $d = 0.5\ell_B$ in the Moore-Read phase and $d = 0.8\ell_B$ in the reconstructed phase according to Ref. [43]. Their fitting exponents are $\eta \simeq 0.658$ and $\eta \simeq 0.599$, respectively. In all cases, the η decreases as decreasing the strength of the confinement potential (increasing d in energy spectrum or increasing R_A in ES before reconstruction). However, it is known [44,45] that the neutral edge mode has one order lower velocity or excitation energy than that of charge mode. From the α_{xy} as labeled by arrow in Fig. 4(d), the low-temperature behaviors are dominated near the scale $k_BT \sim 0.01$, which has the same order of the excited energy for neutral mode as labeled in Fig. 4(b). Therefore, for the non-Abelian FQH state, the Majorana neutral edge mode has much more significant contribution in thermoelectric conductivity and could be more easy to be detected in the low-temperature thermal Hall experiments [22,23].

In addition to the scaling behavior in low temperature, the edge confinement also has effects on the value of α_{xy} itself. In Fig. 5, we plot the ground-state angular momentum and α_{xy} as a function of the confinement parameter d/ℓ_B. Two temperatures are considered. The $M_{\rm tot}$ is the total angular momentum of the ground state which is $3N_e(N_e-1)/2$ for Laughlin state. While increasing d, the electrons firstly stay stably in FQH phase and then form stripes at the edge which is accompanied with a jump of $M_{\rm tot}$ [8,11]. If we treat the $M_{\rm tot}$ as the ground state quantum number, the jumps in $M_{\rm tot}$ correspond to ground-state phase transitions and each $M_{\rm tot}$ could be treated as a phase. It is interesting to see that in the Laughlin phase for $d < 1.35\ell_B$, thermoelectric Hall conductivity α_{xy} is smaller than that of the reconstructed phase. This is because the edge reconstruction $d > 1.35\ell_B$ induces more edge modes and thus make more contributions to the thermal transport. Moreover, the α_{xy} has maximum at the phase transition and minimum at the center of each phases. As the temperature increasing, the structure of α_{xy} is gradually erased by thermal excitations.

IV. DISCUSSIONS AND CONCLUSIONS

In this work, we study the thermoelectric Hall conductivity of the FQH system in disk geometry, especially its low-temperature behaviors. Because of the presence of gapless edge mode, the low-temperature behaviors of α_{xy} in disk geometry are similar to that of the gapless composite Fermi liquid state on a torus. Because the edge spectrum could be changed by tuning the strength of the background confinement in energy spectrum or the area of subsystem in the bipartition ES, the scaling exponent η of $\alpha_{xy} \sim T^{\eta}$ in low temperature has a strong dependence on the system parameters. Comparing to the results on torus, we find η decreases as decreasing the strength of the confinement potential (increasing d in energy spectrum or increasing R_A in ES before reconstruction). For the dipolar fermions at the magic angle, we verify the Fermi liquid behavior with $\eta \sim 1.0$ after gap closing. For non-Abelian Moore-Read state, we find the Majorana neutral edge mode has more significant contribution to the thermoelectric Hall conductivity and dominates the low-temperature behavior, explaining the reason of the non-Abelian signals appear in the low-temperature thermal Hall experiments.

In conclusion, comparing to the results of the composite Fermi liquids on torus, we find the edge excitations of the FQH states dominate the low-temperature scaling behavior of the $\alpha_{xy} \sim T^{\eta}$. Both the α_{xy} and its scaling exponent η are strongly affected by the edge potential which makes the scaling nonuniversal in low temperature. Introducing more edge modes or the neutral mode with lower excitation energy contributes significantly to α_{xy} at low-temperature thermal Hall transport. In case of the edge reconstruction occurring, the thermoelectric Hall conductivity has a peak which probably could be observed in future experiments.

ACKNOWLEDGMENTS

This work was supported by National Natural Science Foundation of China (Grants No. 12075040 and No. 11974064), the Chongqing Research Program of Basic Research and Frontier Technology (Grant No. cstc2020jcyj-msxmX0890), and the Fundamental Research Funds for the Central Universities under Grant No. 2020CDJQY-Z003.

[1] D. C. Tsui, H. L. Störmer, and A. C. Gossard, Phys. Rev. Lett. **48**, 1559 (1982).

[2] R. B. Laughlin, Phys. Rev. Lett. **50**, 1395 (1983).

[3] C. Nayak, S. H. Simon, A. Stern, M. Freedman, and S. Das Sarma, Rev. Mod. Phys. **80**, 1083 (2008).
[4] S. M. Girvin, A. H. MacDonald, and P. M. Platzman, Phys. Rev. Lett. **54**, 581 (1985).
[5] B. Yang, Z. X. Hu, Z. Papic, and F. D. M. Haldane, Phys. Rev. Lett. **108**, 256807 (2012).
[6] A. Chandran, M. Hermanns, N. Regnault, and B. A. Bernevig, Phys. Rev. B **84**, 205136 (2011).
[7] Z. X. Luo, B. G. Pankovich, Y. Hu, and Y. S. Wu, Phys. Rev. B **99**, 205137 (2019).
[8] X. G. Wen, Int. J. Mod. Phys. B **6**, 1711 (1992).
[9] C. de C. Chamon and X. G. Wen, Phys. Rev. B **49**, 8227 (1994).
[10] A. M. Chang, Rev. Mod. Phys. **75**, 1449 (2003).
[11] X. Wan, K. Yang, and E. H. Rezayi, Phys. Rev. Lett. **88**, 056802 (2002).
[12] X. Wan, E. H. Rezayi, and K. Yang, Phys. Rev. B **68**, 125307 (2003).
[13] S. Jolad and J. K. Jain, Phys. Rev. Lett. **102**, 116801 (2009).
[14] S. Jolad, D. Sen, and J. K. Jain, Phys. Rev. B **82**, 075315 (2010).
[15] M. Cygorek, M. Korkusinski, and P. Hawrylak, Phys. Rev. B **101**, 075307 (2020).
[16] V. Venkatachalam, S. Hart, L. Pfeiffer, K. West, and A. Yacoby, Nat. Phys. **8**, 676 (2012).
[17] S. Takei, B. Rosenow, and A. Stern, Phys. Rev. B **91**, 241104(R) (2015).
[18] Y. N. Obraztsov, Sov. Phys. Solid State **7**, 455 (1965).
[19] S. M. Girvin and M. Jonson, J. Phys. C **15**, L1147 (1982).
[20] D. L. Bergman and V. Oganesyan, Phys. Rev. Lett. **104**, 066601 (2010).
[21] V. Kozii, B. Skinner, and L. Fu, Phys. Rev. B **99**, 155123 (2019).
[22] K. Yang and B. I. Halperin, Phys. Rev. B **79**, 115317 (2009).
[23] M. Banerjee, M. Heiblum, V. Umansky, D. E. Feldman, Y. Oreg, and A. Stern, Nature **559**, 205 (2018).
[24] L. Fu, arXiv:1909.09506.
[25] H. Oji, Phys. Rev. B **29**, 3148 (1984).
[26] N. R. Cooper, B. I. Halperin, and I. M. Ruzin, Phys. Rev. B **55**, 2344 (1997).
[27] D. N. Sheng and L. Fu, Phys. Rev. B **101**, 241101(R) (2020).
[28] N. R. Cooper, Adv. Phys. **57**, 539 (2008).
[29] R. Z. Qiu, S. P. Kou, Z. X. Hu, X. Wan, and S. Yi, Phys. Rev. A **83**, 063633 (2011).
[30] Z. X. Hu, Q. Li, L. P. Yang, W. Q. Yang, N. Jiang, R. Z. Qiu, and B. Yang, Phys. Rev. B **97**, 035140 (2018).
[31] W. Q. Yang, Q. Li, L. P. Yang, and Z. X. Hu, Chin. Phys. B **28**, 067303 (2019).
[32] A. Sterdyniak, A. Chandran, N. Regnault, B. A. Bernevig, and P. Bonderson, Phys. Rev. B **85**, 125308 (2012).
[33] J. Dubail, N. Read, and E. H. Rezayi, Phys. Rev. B **85**, 115321 (2012).
[34] I. D. Rodriguez, S. H. Simon, and J. K. Slingerland, Phys. Rev. Lett. **108**, 256806 (2012).
[35] M. A. Nielsen and I. L. Chuang, *Quantum Computation and Quantum Information* (Cambridge University Press, Cambridge, 2000).
[36] A. Kitaev and J. Preskill, Phys. Rev. Lett. **96**, 110404 (2006).
[37] H. Li and F. D. M. Haldane, Phys. Rev. Lett. **101**, 010504 (2008).
[38] F. D. M. Haldane, Phys. Rev. Lett. **51**, 605 (1983).
[39] B. A. Bernevig and F. D. M. Haldane, Phys. Rev. Lett. **100**, 246802 (2008).
[40] B. A. Bernevig and F. D. M. Haldane, Phys. Rev. Lett. **101**, 246806 (2008).
[41] G. Moore and N. Read, Nucl. Phys. B **360**, 362 (1991).
[42] S. H. Simon, E. H. Rezayi, and N. R. Cooper, Phys. Rev. B **75**, 195306 (2007).
[43] X. Wan, Z. X. Hu, E. H. Rezayi, and K. Yang, Phys. Rev. B **77**, 165316 (2008).
[44] Z. X. Hu, E. H. Rezayi, X. Wan, and K. Yang, Phys. Rev. B **80**, 235330 (2009).
[45] N. Jiang and Z. X. Hu, Phys. Rev. B **94**, 125116 (2016).